

## Article

# Effect of Chemical Warm Mix Additive on the Properties and Mechanical Performance of Recycled Asphalt Mixtures

Firas Barraj <sup>1</sup>, Jamal Khatib <sup>1,2,\*</sup>, Alberte Castro <sup>3</sup> and Adel Elkordi <sup>1,4</sup>

<sup>1</sup> Faculty of Engineering, Beirut Arab University, Beirut 11-5020, Lebanon; f.barraj@bau.edu.lb (F.B.); a.elkordi@bau.edu.lb (A.E.)

<sup>2</sup> Faculty of Science and Engineering, University of Wolverhampton, Wolverhampton WV1 1LY, UK

<sup>3</sup> Department of Agroforestry Engineering, Transportation Infrastructures and Engineering, Higher Polytechnic School of Engineering, University of Santiago de Compostela, Campus University s/n, 27002 Lugo, Spain; alberte.castro@usc.es

<sup>4</sup> Department of Civil and Environmental Engineering, Faculty of Engineering, Alexandria University, Alexandria 21511, Egypt

\* Correspondence: j.khatib@bau.edu.lb

**Abstract:** Newer technologies such as warm mix asphalt (WMA) and reclaimed asphalt pavement (RAP) have gained international approval and have been considered as appropriate solutions that support the sustainability goals of the highway sector. However, both technologies present some shortcomings. The lower mixing and compaction temperatures of WMA reduce the binder aging and the bond between the aggregates and the coating binder, thus resulting in less rutting resistance and higher moisture susceptibility. On the other hand, RAP mixes tend to be stiffer and more brittle than conventional hot mix asphalt (HMA) due to the effect of aged binder. This tends to increase the crack propagation distresses. In an attempt to overcome their individual shortcomings, this study investigated the new concept of a combined WMA-RAP technology. The chemical WMA additive Rediset LQ1102CE was utilized with mixtures incorporating low (15%), medium (25%), and high (45%) RAP contents. Dynamic modulus (DM) and flow number (FN) tests were conducted to investigate the effect of Rediset on the behavior of RAP mixtures. The dynamic modulus  $|E^*|$  mastercurves were developed using the sigmoidal model and Frankén model was used to fit the accumulated permanent deformation curve. The results of this study showed that Rediset addition improved the cracking resistance of RAP mixtures. However, the rutting resistance was reduced but kept within the acceptable range except for mixtures containing low RAP content.

**Keywords:** reclaimed asphalt pavement; warm mix; recycled; sustainability; dynamic modulus; energy consumption



**Citation:** Barraj, F.; Khatib, J.; Castro, A.; Elkordi, A. Effect of Chemical Warm Mix Additive on the Properties and Mechanical Performance of Recycled Asphalt Mixtures. *Buildings* **2022**, *12*, 874. <https://doi.org/10.3390/buildings12070874>

Academic Editor: Pengfei Liu

Received: 20 May 2022

Accepted: 14 June 2022

Published: 21 June 2022

**Publisher's Note:** MDPI stays neutral with regard to jurisdictional claims in published maps and institutional affiliations.



**Copyright:** © 2022 by the authors. Licensee MDPI, Basel, Switzerland. This article is an open access article distributed under the terms and conditions of the Creative Commons Attribution (CC BY) license (<https://creativecommons.org/licenses/by/4.0/>).

## 1. Introduction

Newer technologies such as warm mix asphalt (WMA) and reclaimed asphalt pavement (RAP) have gained international approval and have been considered as appropriate solutions that support the sustainability goals of the highway sector. Warm mix technology lowers the production and compaction temperatures which contributes to a reduction in the amount of greenhouse gases emitted and energy consumption [1,2]. Reclaimed asphalt technology promotes the recycling of old pavement materials to be used as a replacement of virgin binder and aggregates for the production of new asphalt mixtures. Moreover, RAP technology leads to the preservation of non-renewable resources, reduction of production costs, and other economic and environmental benefits [3]. However, both technologies present some shortcomings. The lower mixing and compaction temperatures of WMA reduce the binder aging and the bond between the aggregates and the coating binder, thus resulting in less rutting resistance and higher moisture susceptibility [4–6]. On the other hand, RAP mixes tend to be stiffer and more brittle than conventional HMA mixtures due

to the effect of aged binder. Typically, in recycled pavement mixtures, with the admixing of aged asphalt, the blended asphalt is harder, has higher elasticity, and lower viscosity. The high-temperature performance improves, but the low-temperature performance worsens [7,8]. This tends to increase the crack propagation distresses [9,10]. In order to overcome these shortcomings, WMA-RAP technology has been investigated [11,12]. The aged binder of RAP might efficiently compensate for the soft warm mix binder, so that the fatigue life of RAP mixes gets extended and the rutting performance of WMA mixes is maintained. Ultimately, the most desirable feature of WMA-RAP mixes is the reduction in production and compaction temperatures while incorporating increased proportion of RAP leading to overall saving in energy and economical cost without compromising on the properties of the bituminous mix [13].

A number of studies have been conducted in recent years to understand the performance of WMA-RAP mixtures. Oliveira et al. [14] indicated that the rutting resistance of HMA and RAP mixes was improved with the addition of a surfactant-based additive, however, the effect was mostly recognized in RAP mixtures. Gungat et al. [15] used a multiple stress creep and recovery (MSCR) test to investigate the effect of RH-WMA (combination of polyethylene and wax) on asphalt mixtures incorporating 30, 40, and 50% RAP, and noticed an improvement in the rutting resistance with the increase in RAP content. Zhao et al. [16] conducted asphalt pavement analyzer, Hamburg wheel tracking, and flow number tests on asphalt samples mixed with a foaming WMA additive, and incorporating RAP contents of 15% and 30%. They found that increased RAP content contributes to a decrease in the rut depth regardless of the source of reclaimed materials. Similar findings were reported by Xie et al. [17]. Table 1 presents the effect of different WMA additives on the rutting performance of mixtures containing RAP.

**Table 1.** Effect of WMA additives on the rutting resistance of RAP mixtures.

Reference	Additive Type	Additive Dosage %	RAP %	Mix Design Characteristics	Rutting Resistance of WMA-RAP Mixture
Behbahani et al., 2017 [18]	Organic additive (Sasobit)	3	25, 50, 70	Dense graded mixtures prepared according to Marshall method and designed for Va of 4%	Sasobit addition showed better rutting resistance than Zycotherm Increase
	chemical anti-stripping agent (Zycotherm)	3			
Lu et al., 2016 [19]	Chemical additive (Evotherm 3G)	0.5	25, 50, 70	Dense graded mixtures compacted using the gyratory compactor following Australian standards at optimum binder content for Va of 4%	Evotherm 3G showed better rutting resistance than Sylvaroad TM RP 1000
	Sylvaroad TM RP 1000 *	2			
Guo et al., 2016 [20]	Surfactant additive (SI)	5.3	20, 40	Dense graded mixtures prepared according to Marshall method for a Va of 4.5%	SI WMA-RAP showed better rutting resistance than Evotherm DAT WMA-RAP
	Chemical additive (Evotherm DAT)	11			
Kim et al., 2017 [21]	Organic (Sasobit)	1.5	35	Dense graded mixtures compacted using Superpave gyratory compactor according to AASHTO T 342-11 for Va ranging from 4.7% to 7.4%	Evotherm and Sasobit WMA-RAP presented the same rutting resistance, while Advera additive cause a relatively poor performance
	Chemical (Evotherm)	0.5			
	Foaming (Advera)	[0.25]			
Sharkawy et al., 2016 [22]	Organic wax (Sasobit)	1.5; 3	15	Dense graded mixtures prepared according to Marshall method for Va between 3% and 5%	Rutting depth decreased by 11.91% if Sasobit additive content increased by 1.5%
Valdes-Vidal et al., 2018 [23]	Foaming Technique (Zeolite)	[0.3]; [0.6]	20	Semi-dense asphalt mixtures prepared following Marshall method according to Chilean standard for Va ranging between 4.5% and 5.3%.	The rutting depth of Zeolite with 0.6% content was 5 mm shallower than that of Zeolite with 0.3%

**Note:** [-] indicates that dosage % is by weight of the mix while others are by weight of the binder; \* product made from Crude Tall Oil and Crude Sulphate Turpentine.

In addition to the rutting potential of WMA-RAP mixtures, the fatigue under repetitive loading and low temperature cracking need to be assessed. In that context, Das et al. [24] conducted dynamic modulus (DM), indirect tensile (IDT), and bending beam rheometer (BBR) tests to measure the stiffness, creep compliance, and tensile strength of WMA-RAP asphalt samples and showed that water foaming WMA and asphaltene B additives had no effect on the fatigue and thermal cracking performance of RAP mixes. Gabchi et al. [25] found that Zeolite-based additives (ZTWM, CHWM-B, and CHWM-S) enhance the creep compliance of RAP mixtures at  $-18\text{ }^{\circ}\text{C}$  which implies a better stress relaxation and a better thermal cracking resistance for WMA-RAP. Vaitkus et al. [26] reported a decline in the cracking performance of WMA-RAP mixtures when Sasobit dosage exceeds 2%. In another study by Singh et al. [27], the results of the semi-circular bending (SCB) testing indicated that the addition of Ft-wax additive reduced the fracture resistance of RAP mixes. Zhao et al. [16] found that the cracking performance of asphalt mixtures containing up to 30% RAP content could be improved by the WMA foaming technology; however, when 30% threshold is exceeded, the performance is compromised.

Another concern regarding WMA-RAP mixtures is its moisture susceptibility, especially for foamed techniques that work by injecting water to lower the virgin binder viscosity. Low mixing temperature feature of WMA, non-ductile RAP binder, and aggregate stripping concerns of RAP technology are main factors that create the necessity to investigate the moisture susceptibility of WMA-RAP produced mixtures. For this reason, to assess WMA additive impact, Frigio et al. [28] conducted indirect tensile strength ITS, Cantabro, SCB, and repeated indirect tensile tests on mixes containing 15% of RAP and using different WMA additives and found that the chemical additive provides acceptable resistance to moisture while the organic wax and zeolite performed poorly. The chemical additive performed best because of the inherent antistripping capabilities. Moreover, Guo et al. [29] indicated that the short-term aged WMA-RAP mixtures provided higher tensile ratio TSR moisture resistance than the corresponding RAP mixture. However, TSR values were drastically reduced after long-term aging.

Further studies should be conducted to characterize the effect of the diversity of available WMA additives on the properties and mechanical performance of asphalt mixtures produced through WMA-RAP technology in order to determine the best additive and with which RAP content. In this regard, the work of this paper addresses this goal and discusses the impact of a chemical WMA additive (Rediset LQ1102CE<sup>®</sup>) on the performance of asphalt mixtures incorporating low (15%), medium (25%), and high (45%) RAP contents. The Rediset effect on reclaimed asphalt mixtures needs to be investigated. Rediset additive can be considered as an easy-to-use liquid that not only is a WMA additive, but it also provides an active adhesion that enhances the coating of aggregates and improves the moisture resistance of asphalt mixtures [30,31].

Therefore, the objectives of this paper are to: (a) Determine the effect of the chemical WMA additive Rediset on the dynamic modulus and phase angle properties of the asphalt mixture containing different RAP percentages, (b) evaluate the impact of Rediset addition on the permanent deformation and the fatigue behavior of RAP mixtures, and (c) investigate the correlations between the flow number (FN) and dynamic modulus (DM) results used to characterize the asphalt mix rutting resistance potential.

## 2. Experimental

### 2.1. Materials

Raw materials consisting of limestone aggregates, unmodified binder with a performance grade PG 64-22, and RAP aggregates from one single source were used in the fabrication of all the mixtures of the study. The average binder contents of fine and coarse RAP fractions determined following the centrifugal extraction method of ASTM D2172M and the average particle size distribution of extracted aggregates from each RAP stockpile are illustrated in Table 2 and Figure 1. The evaluation of the recovered binder of recycled pavement materials showed RAP binder to be graded at PG 88-4. Increased performance

grade for RAP binder properties is the result of asphalt oxidation, volatilization, and steric hardening, which are involved in the asphalt's long-term aging process [32].

**Table 2.** Average binder content of coarse and fine RAP laboratory samples.

Sample ID	1	2	3	4	Average	Standard Deviation
RAP + 4.75 mm	3.66	3.50	3.64	4.05	3.71	0.236
RAP − 4.75 mm	5.01	5.40	4.98	5.17	5.14	0.192

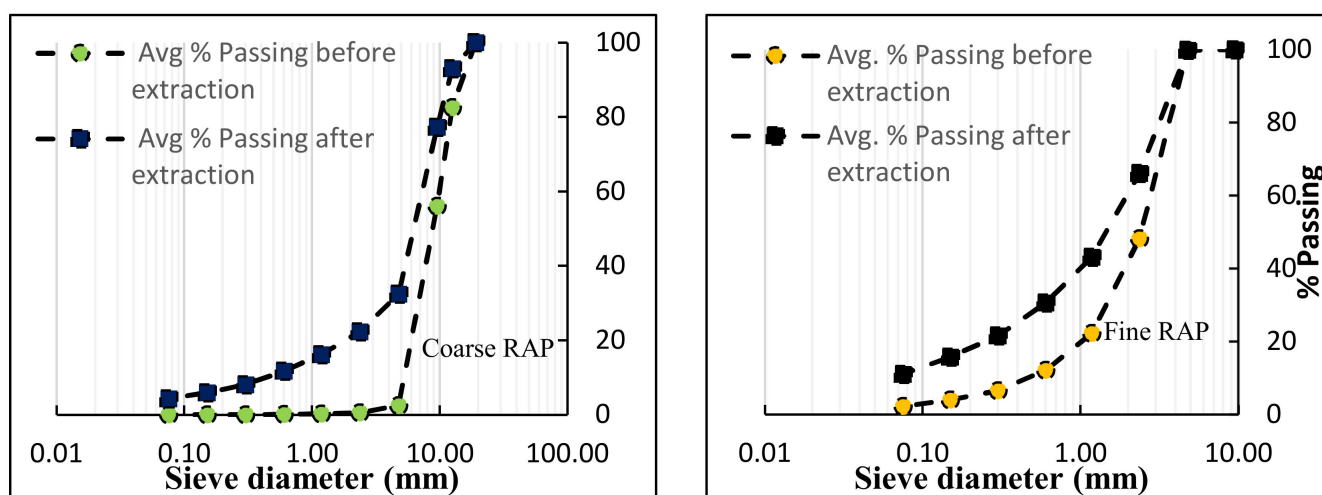


**Figure 1.** Particle size distribution of RAP fractions before and after extraction of binder (BE and AE).

The binder from RAP was assumed to be totally blended with the virgin binder as recommended by Superpave Technical Report [33]. Therefore, the amount of RAP binder and the after extraction (AE) curves of RAP aggregates for both RAP fractions were considered in the mix design. Binder replacement ratios of 13.02%, 21.6%, and 38.37% were found for mixes with 15%, 25%, and 45% RAP contents, respectively. It should be noted that the mixing conditions were optimized as suggested by Abed et al. [34] to maximize the degree of blending DOB between virgin and RAP binders so that the full blending assumption is reasonable. In this context, the mixing time was extended to 6 min for all mixes and the mixing temperature was maintained at 135 °C for warm asphaltic mixtures. For WMA-RAP mixtures prepared with reduced temperatures, the chemical WMA additive Rediset LQ1102CE<sup>®</sup>, developed by Akzonobel (Amsterdam, The Netherlands) and which comes in the form of a liquid, was utilized. This type of additive reduces the friction between the aggregate and the asphalt binder that is coating it, improving the workability of AC mixtures during its production and compaction processes.

## 2.2. Preparation of Asphalt Mixtures

In this study, six AC mixtures are assessed having aggregate gradation with a nominal maximum aggregate size (NMAS) of 12.5 mm designed to meet the control points criteria's of Superpave (SP-2) [35] as illustrated in Figure 2. The labels "HR15", "HR25", "HR45", "WR15", "WR25", and "WR45" are used in the upcoming sections to designate, respectively, HMA mix with 15% (low RAP content), 25% (medium RAP content), and 45% (high RAP content), 15% (low RAP content + Rediset), 25% (medium RAP content + Rediset), and 45% (high RAP content + Rediset).

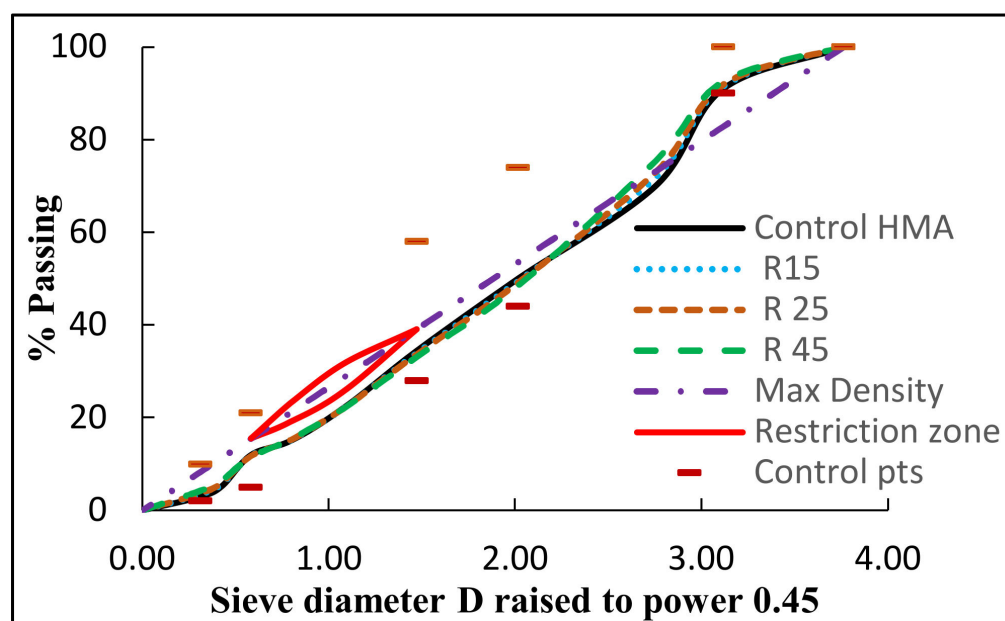


Figure 2. Gradation selected for asphalt mixtures.

It is worth noting that in order to obtain grading curves for mixes containing RAP that are close to a control gradation, the proportions for coarse and fine RAP materials in the mixture were adjusted according to the percentage of RAP incorporation as shown in Table 3.

Table 3. Coarse and fine RAP proportions in RAP and WMA-RAP mixes.

% RAP in Mix	15%	25%	45%
% Coarse fraction	11.82	19.71	35.47
% Fine fraction	3.18	5.29	9.53

#### Mix Design and Compaction

The mix design for “HR15”, “HR25”, and “HR45” mixtures of the study was conducted to determine the optimum binder content OBC (% by weight of the mix) that provides a design air voids  $V_a$  of 4%. Then, the WMA-RAP mixes were designed by validating the OBC that was determined for each of the corresponding HR mixes. In order to design a WMA-RAP mix with a specific volume of air voids, three different factors can be varied: compaction temperature, asphalt content, and/or WMA additive dosage. The same OBC of HR mix was used for the corresponding WMA-RAP mix to obtain similarity of volumetric properties so that a comparable performance can be achieved between HR and its corresponding WR mix [36]. Moreover, this study adopted the same temperature reduction of 25 °C for both the mixing and compaction of the WMA-RAP mixes. The supplier of Rediset additive recommends a dosage between 0.3% and 0.7% by weight of the binder and a reduction range in the mixing and compaction temperatures between 20–40 °C. The level of temperature reduction was targeted to satisfy the condition of ensuring a full coating of the aggregates and a 4.0% air voids for the same compaction effort used for HMA. For each WMA-RAP mix, different Rediset dosages were tried such that they fell within the range recommended by the supplier in order to determine the appropriate dosage for each level of RAP incorporation. A summary of the mix design parameters for all mixtures is shown in Table 4.

**Table 4.** Summary of mix design results for HR and WR mixes.

Mix	HR15	HR25	HR45	WR15	WR25	WR45	Superpave Criteria
<b>OBC</b>	4.6	4.62	4.68	4.6	4.62	4.68	
<b>Va %</b>	4.0	4.0	4.0	4.1	3.94	4.02	4
<b>VMA %</b>	14.01	14.0	14.125	14.05	14.01	14.09	14% min
<b>VFA%</b>	71.58	71.39	71.65	71.45	71.4	71.55	65–75
<b>% Gmm at Nini</b>	85.77	85.56	85.14	85.95	85.88	85.64	89% max
<b>% Gmm at Nmax</b>	97.43	96.99	97.48	97.63	97.29	97.73	98% max
<b>Rediset dosage</b>	-	-	-	0.5	0.4	0.31	
<b>% Dust proportion (DP)</b>	0.7	0.71	0.7	0.72	0.71	0.71	0.7–1.2
<b>Mixing temperature °C</b>	160	160	160	135	135	135	
<b>Compaction temperature °C</b>	150	150	150	125	125	125	

The results of the mix design showed that the volumetric properties for HR and WR mixes are comparable and acceptable according to Superpave mix design criteria. Moreover, it is seen that the optimum binder content to achieve air voids volume Va of 4% did not vary by more than 0.08% between the mixes with low and high RAP contents indicating efficient blending between virgin and RAP binder occurred at the chosen mixing temperature.

### 2.3. Testing

#### 2.3.1. Complex Modulus Test

The complex modulus test ( $E^*$ ) is an unconfined test conducted to characterize the stiffness measured in term of the dynamic modulus  $|E^*|$ , and viscoelastic behavior exhibited by the phase angle  $\Phi$  of asphalt mixtures over a range of different temperatures and loading frequencies. The National Cooperative Highway Research Program (NCHRP) report 547 of the NCHRP Project 9–19 recommended  $|E^*|$  as one of the most promising simple performance tests for rutting and fatigue cracking specification because of its significant correlation with these distresses [37]. Higher  $|E^*|$  at small, intermediate, and large frequencies correlated, respectively, to better rutting resistance, worst fatigue, and worst thermal cracking resistance and vice versa [38]. In this test, asphalt concrete (AC) samples with height of 150 mm and diameter of 100 mm are subjected to repetitive sinusoidal dynamic compressive axial load (stress) as shown in Figure 3. The stress amplitude is controlled to produce a recoverable strain not exceeding a maximum amplitude of 70 microstrains to keep the material response in the linear viscoelastic range [39]. For this study, three replicates of each AC mixture were tested at three temperatures, 5, 20, and 40 °C, and six loading frequencies, 20, 10, 5, 1, 0.5, and 0.1 Hz, following the Aashtoo T 342-11 protocol. The averages of the  $|E^*|$  and  $\Phi$  of the three specimens at each temperature/frequency combination were calculated. Then, the dynamic modulus and phase angle mastercurves were constructed by applying the time temperature superposition (TTS) principle at a reference temperature of 20 °C.

The dynamic modulus  $|E^*|$  mastercurves were developed using the sigmoidal model of Equation (1) as a function of the reduced frequency  $f_r$  which in turn is a function of real frequency  $f$  and temperature  $T$  as shown in Equations (2) and (3).

$$\text{Log} (|E^*|) = \delta + \frac{\alpha}{1 + e^{\beta + \gamma \log(f_r)}} \quad (1)$$

$$\log f_r = \log f + \log (a_T) \quad (2)$$

$$\text{Log} (a_T) = a_1 T^2 + a_2 T + a_3 \quad (3)$$

where  $\delta$ ,  $\alpha$ ,  $\beta$ , and  $\gamma$  are regression constants found by numerical minimization between measured and fitted values of  $\log |E^*|$ .  $\delta$ ,  $\alpha$ , ( $\beta$  and  $\gamma$ ) represent, respectively, the minimum value of  $|E^*|$ , vertical span of the modulus function, and shape parameters, and  $a_1$ ,  $a_2$ , and  $a_3$  represent regression coefficients of the polynomial model used to fit the shift factor function  $\log(a_T)$  at any particular temperature.

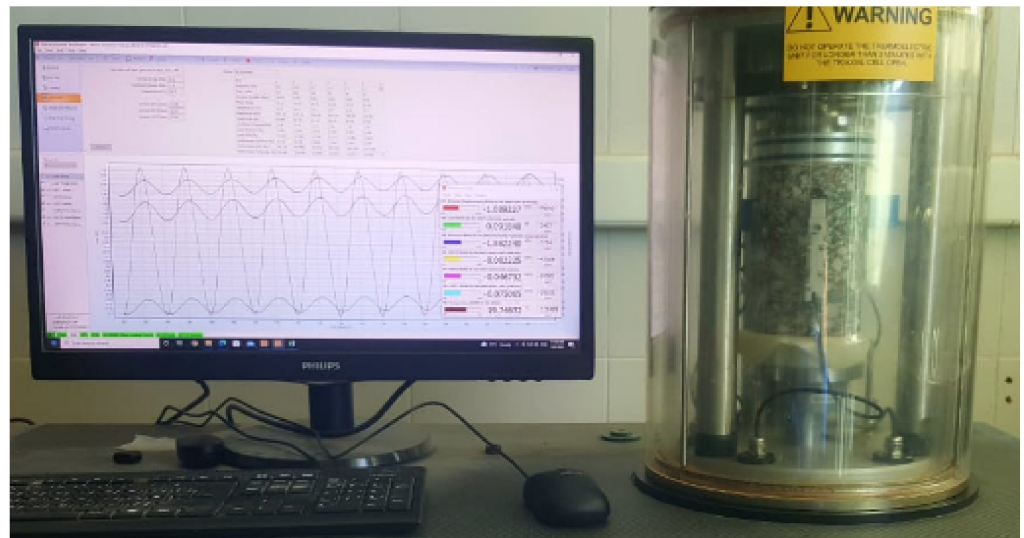


Figure 3. Complex modulus testing in the asphalt mixture performance tester (AMPT).

### Dynamic Modulus Mastercurves

Figure 4 presents an example of construction of the mastercurve of the RAP mixture “HR15” by shifting measured  $|E^*|$  values horizontally over the frequency axis.

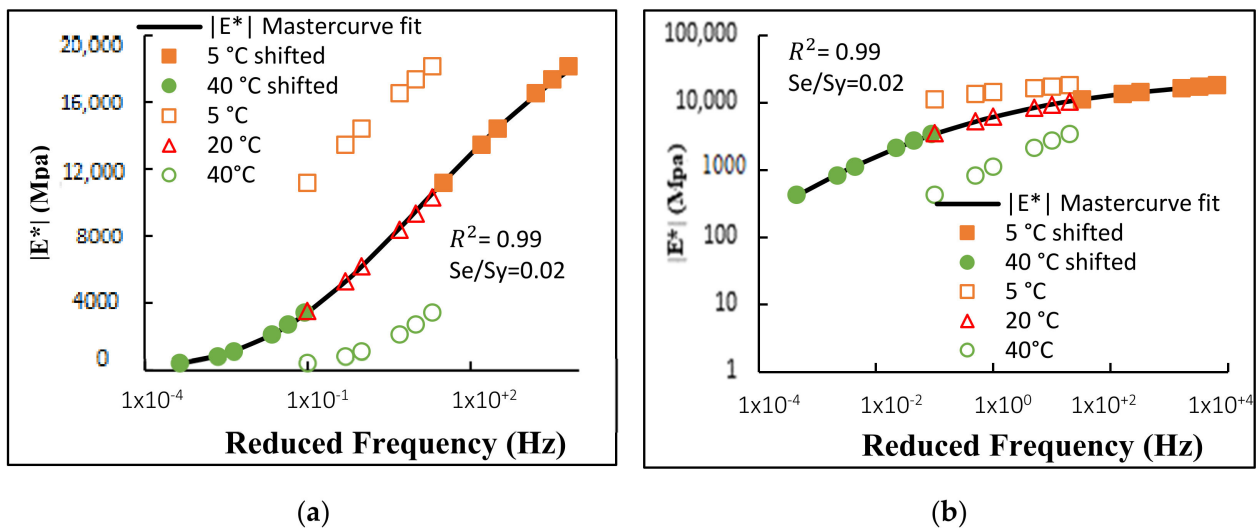


Figure 4. Dynamic modulus mastercurve of RAP mix “HR15” at 20 °C in (a) semi-log scale, (b) log-log scale.

### Phase Angle Mastercurves

The phase angle  $\Phi$  is defined as the delay between the applied peak stress and the peak strain response under cycling loading [37].  $\Phi$  is needed to calculate the storage and the loss modulus components of the complex modulus. It also provides direct insight into the magnitude of viscous and/or elastic state of the AC mixture. The higher the phase angle measured, the lower is the elasticity of AC, and thus more viscous behavior governs.

$\Phi = 0^\circ$  for a purely elastic material and  $90^\circ$  for a purely viscous material. To construct the  $\Phi$  mastercurve, a similar approach to the  $|E^*|$  mastercurve can be adopted. Moreover, since AC is a thermorheologically simple TRS material [40],  $\Phi$  values measured at a particular temperature can be shifted horizontally to the reference temperature using the same shift factors found while developing  $|E^*|$  mastercurve.

Figure 5 shows a typical  $\Phi$  versus  $f_r$  graph for the RAP mixture “HR15” at a reference temperature of  $20^\circ\text{C}$ .

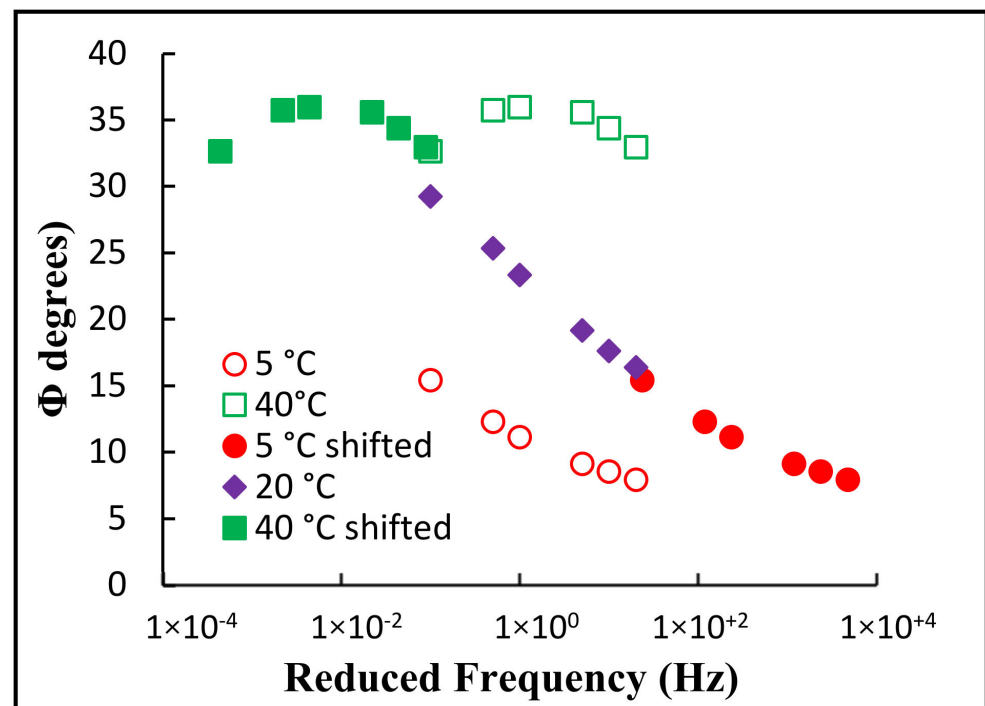


Figure 5. Phase angle construction for the “HR15” mixture.

It is recognized that the shifted data of  $\Phi$  forms approximately a single smooth curve, indicating that the shift factors from  $|E^*|$  can be successfully used to construct the  $\Phi$  mastercurve. Very few models exist in the literature intended to fit a  $\Phi$  mastercurve. The most common are the Booji and Thoone [41] approximate model, and its modified version proposed by Yang and You [42] expressed in Equations (4) and (5), respectively.

$$\Phi(f_r) = -90 \alpha \gamma \frac{e^{\beta + \gamma \log(f_r)}}{\left(1 + e^{\beta + \gamma \log(f_r)}\right)^2} \quad (4)$$

$$\Phi(f_r) = -c \cdot 90 \alpha \gamma \frac{e^{\beta + \gamma \log(f_r)}}{\left(1 + e^{\beta + \gamma \log(f_r)}\right)^2} \quad (5)$$

where  $\Phi(f_r)$  is the phase angle in degrees,  $f_r$  is the reduced frequency in Hz,  $\alpha$ ,  $\beta$ ,  $\gamma$  are the fitting parameters found in the sigmoidal function of the dynamic modulus presented in Equation (1), and  $c$  is a regression parameter found by numerical minimization between measured and fitted values of  $\Phi$ . As shown in Figure 6, the  $\Phi$  mastercurve fitted using the aforementioned models lacked some accuracy in predicting the phase angle. Thus, another modification was proposed to Yang and Lou model as expressed in Equation (6).

$$\Phi(f_r) = k_1 [\log(f_r)]^3 + k_2 [\log(f_r)]^2 + k_3 [\log(f_r)] - k_4 \cdot 90 \cdot \alpha \gamma \frac{e^{\beta + \gamma \log(f_r)}}{\left(1 + e^{\beta + \gamma \log(f_r)}\right)^2} \quad (6)$$

where  $k_1, k_2, k_3, k_4$  are constant regression parameters.

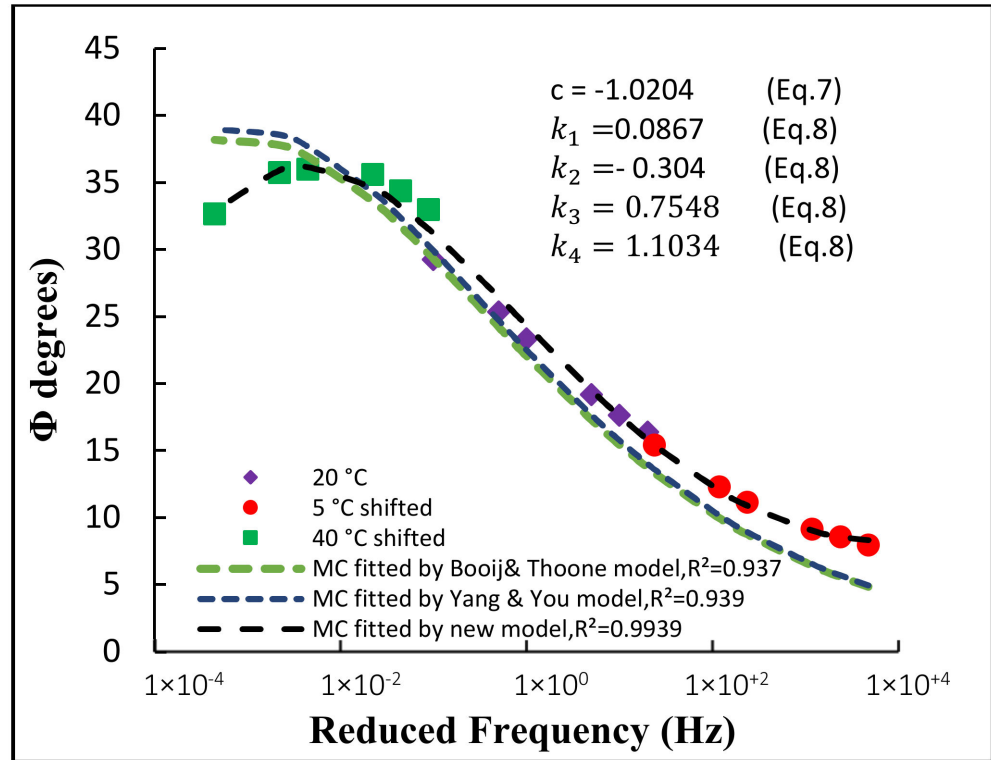
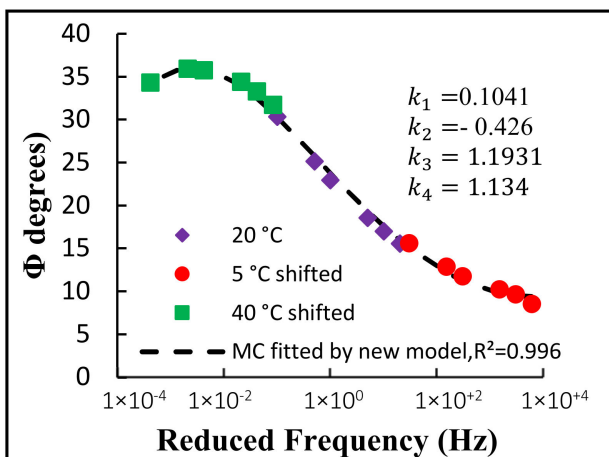
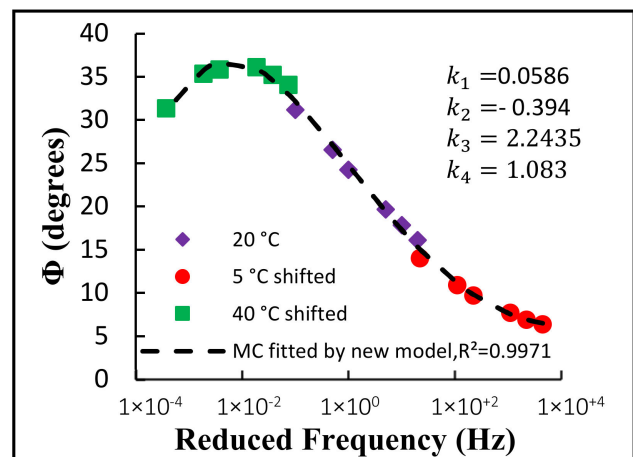


Figure 6. Phase angle mastercurves fitted by the three models for RAP mix “HR15”.

As it can be seen, the proposed model accurately predicted the  $\Phi$  mastercurve of RAP mix “HR15”. Furthermore, Figure 7 illustrates an example of the phase angle mastercurves fitted using Equation (6) for HR and WR mixes. It is observed that good fits are obtained, thus, the phase angle mastercurves of various mixes of the study predicted using Equation (6) were used to analyze the effect of Rediset on the phase angle of mixtures incorporating different RAP percentages.



(a)



(b)

Figure 7. Phase angle mastercurves fitted using Equation (9) for: (a) HR 25%, (b) WR 25%.

### 2.3.2. Flow Number (FN) Test

The flow number test is a simple performance test (dynamic creep and recovery test) introduced by the NCHRP 9–19 Project to assess the rutting potential of asphalt mixes [37].

In this test, AC samples with height of 150 mm and diameter of 100 mm are subjected to haversine compressive cyclic loading, each cycle consisting of a load pulse of 0.1 s long followed by a 0.9 s rest period, to measure the accumulated axial permanent strains as a function of loading cycles. For this study, FN testing was conducted according to Aashtoo T378-17 using a peak amplitude of the repeated axial stress equal to 600 Kpa under a temperature of 53 °C to simulate the pavement surface conditions during summer in regions with hot climate. The test was set to terminate at 10,000 loading cycles or accumulated 7% permanent strain, whichever came first.

Figure 8 shows a typical plot of the accumulation of the permanent strain under a given set of material, load repetitions and environmental conditions. Three zones of permanent deformation are identified: (1) Primary zone, predominantly attributed to volumetric change, in which high initial level of rutting occurs and the rate of plastic deformations decreases as the number of cycles increases; (2) secondary zone, attributed predominantly to volumetric changes in addition to plastic deformations induced by shear stresses, in which a small level of rutting is encountered and the deformation rate is approximately constant with loading cycles; and (3) tertiary zone, predominantly associated with plastic (shear) deformations under no volume change conditions, in which high level of rutting is exhibited and the rate of deformation increases rapidly with loading cycles.

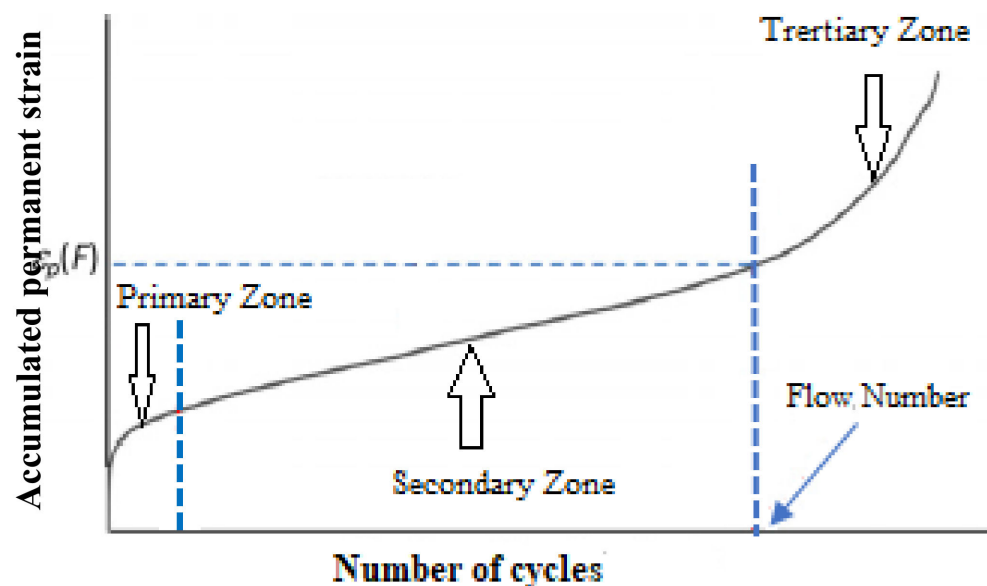


Figure 8. Typical repeated load vs. permanent strain (deformation) behavior of pavement materials [43].

#### Model Used to Identify the Flow Number

The flow number FN is defined as the number of load cycles at which the asphalt mixture reaches the flow point, i.e., the start of the tertiary zone. FN, expressed in cycles, corresponds to the point where the slope of the permanent strain curve reaches a minimum value. A stable and rational approach to determine FN was recommended by Researchers at the Arizona State University (Tempe, AZ, USA) [44], in which the permanent axial strain is initially fitted using the Franken model expressed by Equation (7) below.

$$\epsilon_p = An^B + C(e^{Dn} - 1) \quad (7)$$

where  $\epsilon_p$  is the permanent axial strain,  $n$  is the number of cycles, and  $A$ ,  $B$ ,  $C$ , and  $D$  are regression coefficients found by numerical optimization (minimization of error) between measured and fitted values of permanent strains per each cycle. Once fitted, the first and second derivatives of the Francken model can be easily calculated analytically as shown in

Equations (8) and (9), respectively, and the flow number is located as the cycle where the second derivative changes from negative to positive sign.

$$\frac{d\varepsilon_p}{dn} = ABn^{(B-1)} + CD e^{Dn} \quad (8)$$

$$\frac{d^2\varepsilon_p}{dn^2} = AB(B-1)n^{(B-2)} + CD^2 e^{Dn} \quad (9)$$

An example on the curve fitting of the measured permanent axial strain using the Franken model is illustrated by Figure 9 for one replicate of “HR15” mixture and the flow number FN is determined at 294 cycles.

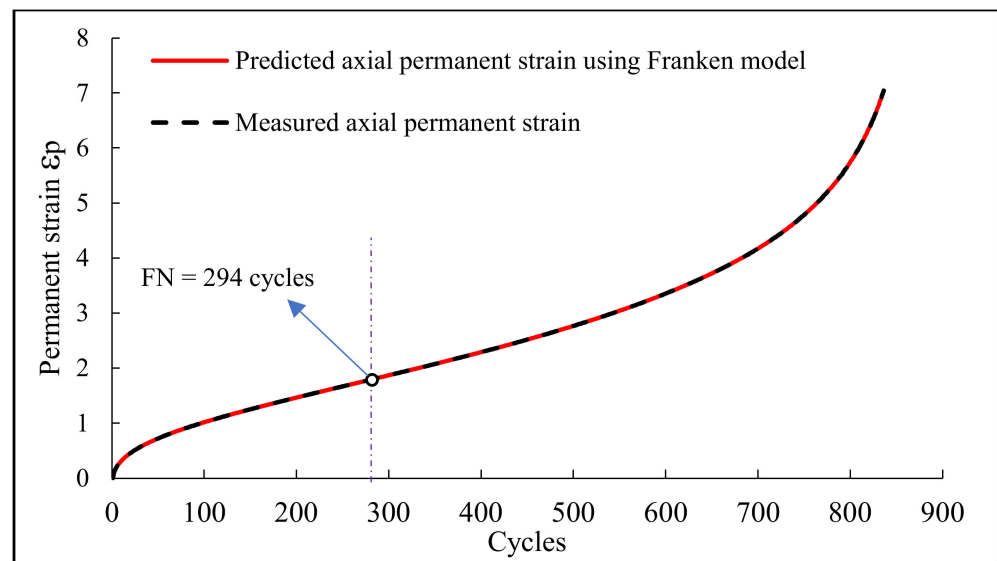


**Figure 9.** Flow number determination using Franklin model for fitting the measured accumulated permanent strain (%) curve for one replicate of the “HR15” mixture.

Although the flow number has been widely accepted as an indicator of the rutting resistance [37], Zhang et al. [45] suggested that a FN Index parameter provides more balanced evaluation of the rutting performance of asphalt mixtures since it takes into consideration both the strains and the number of load repetitions endured till entering the tertiary flow. FN index equation is expressed by Equation (10) below. For performance analysis, higher values of FN indicate better rutting resistance whereas higher FN index values indicate a worst rutting resistance of AC mixtures.

$$\text{FN Index} = \frac{\varepsilon_p}{\text{FN}} \quad (10)$$

### 3. Results and Analysis

#### 3.1. Mastercurves Parameters

For all mixes of the study, the summary of the fitting parameters associated with the functions of  $|E^*|$ ,  $\log a$ , and  $\Phi$  is presented in Table 5.

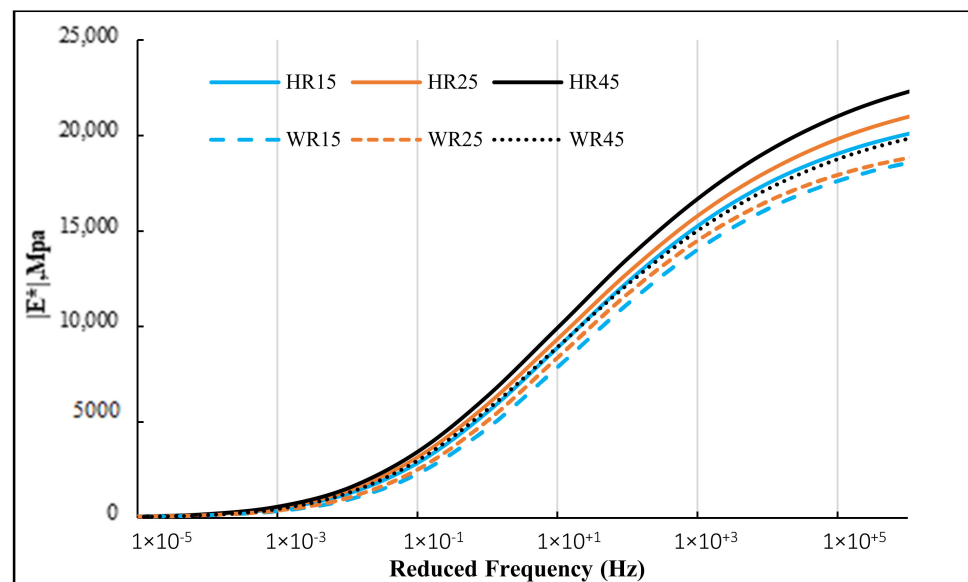
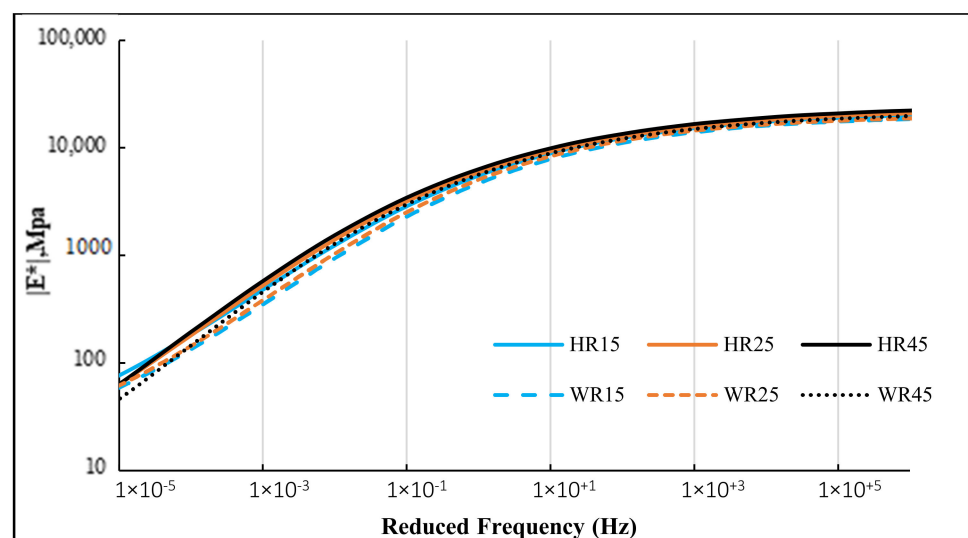
$R^2$  statistics (above 0.99) indicates an excellent curve fitting of the dynamic modulus and phase angle mastercurves to measured data utilizing the sigmoidal model given in Equation (1) and the polynomial shift factor function expressed in Equation (2), as well as the modified phase angle expression of Equation (6).

**Table 5.** Summary of mastercurve (MC) fitting parameters and statistics for various AC mixtures.

Mix Type	E*  MC Parameters					Log at Versus T Function Parameters				Φ MC Parameters				
	δ	α	β	γ	R <sup>2</sup>	a <sub>1</sub>	a <sub>2</sub>	a <sub>3</sub>	R <sup>2</sup>	k <sub>1</sub>	k <sub>2</sub>	k <sub>3</sub>	k <sub>4</sub>	R <sup>2</sup>
HR 15	0.9162	3.4227	−1.5560	−0.4976	0.9994	0.0012	−0.1871	3.2797	1.0000	0.0868	−0.3042	0.7548	1.1035	0.9939
HR 25	0.3057	4.0590	−1.7698	−0.4616	0.9994	0.0013	−0.1983	3.4372	1.0000	0.1041	−0.4267	1.1931	1.1342	0.9965
HR 45	0.0245	4.3699	−1.8576	−0.4464	0.9997	0.0013	−0.1946	3.3768	1.0000	0.1416	−0.5874	0.8227	1.1285	0.9975
WR15	0.9676	3.3350	−1.4544	−0.5208	0.9996	0.0013	−0.1936	3.3341	1.0000	0.0423	−0.1701	0.7423	1.0473	0.9973
WR25	0.9649	3.3405	−1.5196	−0.527	0.9991	0.001	−0.1813	3.2268	1.0000	0.0933	−0.3806	0.5469	1.0610	0.9971
WR45	−0.0449	4.3838	−1.8692	−0.4636	0.9991	0.0011	−0.1885	3.327	1.0000	0.1217	−0.8457	2.1842	1.1564	0.9909

### 3.2. Dynamic Modulus Results

Figures 10 and 11 show the dynamic modulus mastercurves of diverse mixes of the study in log-log and semi-log scale, respectively.

**Figure 10.** Dynamic modulus mastercurves in semi-log scale.**Figure 11.** Dynamic modulus mastercurves in log-log scale.

A quick analysis of the plots indicated that the higher the RAP content, the higher is the  $|E^*|$  of the mixture for both RAP and WMA-RAP technology. Moreover, the values of modulus of all HR mixes are higher than those corresponding to WR mixes. Except  $f_r$  of  $10^{-5}$  Hz, from the largest to smallest, over the full analyzed frequency range,  $|E^*|$  of the mixtures can be mostly ranked as follow: HR45, HR25, HR15, WR45, WR25, and finally WR15.

Specifically, the results showed that the addition of Rediset additive reduces  $|E^*|$  of the corresponding HR mix at both high and low reduced frequencies. Because of the strong correlation between  $|E^*|$  and the rutting and fatigue distresses [37], this reduction in  $|E^*|$  implies that the addition of Rediset might affect the performance of AC mixtures.

### Effect of Rediset on $|E^*|$ According to RAP Content

To highlight the effect of Rediset on each RAP content separately, the reduction (%) in  $|E^*|$  against the reduced frequency is presented in Figure 12. For analysis purposes, the frequency range of  $|E^*|$  mastercurves is decomposed into three arbitrary zones: (1) lower range from  $10^{-5}$  to  $10^{-2}$  Hz, middle range from  $10^{-2}$  to  $10^{+2}$  Hz, and a higher range from  $10^{+2}$  to  $10^{+5}$  Hz. It is worth noting that the behavior of AC mixtures at the lower, middle, and higher frequency ranges correspond to its behavior at regions with high, normal (operational), and low temperature ranges.

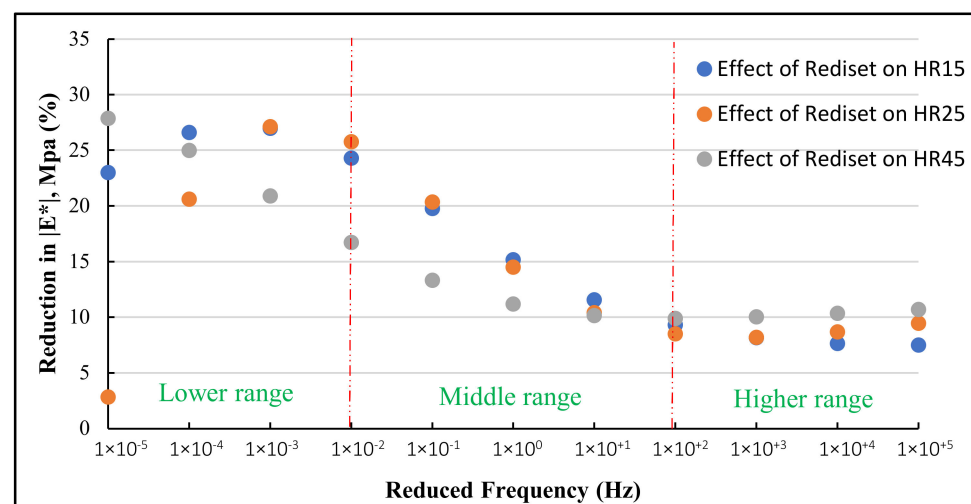


Figure 12. Effect of Rediset on  $|E^*|$  of mixtures with RAP.

For HMA mixtures incorporating low RAP content (HR15), higher reduction due to Rediset addition occurred in the lower frequency range compared to the middle and higher range. This reduction is significant and increased from 22.98% at  $10^{-5}$  Hz to a maximum of 26.97% at  $10^{-3}$  Hz then decreased to 24.27% at  $10^{-2}$  Hz. In the middle frequency range, the reduction in  $|E^*|$  decreased from 24.27% at  $10^{-2}$  Hz to 9.32% at  $10^{+2}$  Hz. In the higher frequency range, the reduction in  $|E^*|$  is almost constant and not significant ranging between 9.32% at  $10^{+2}$  Hz and 7.5% at  $10^{+5}$  Hz.

For HMA mixtures incorporating medium RAP content (HR25), the reduction is slight at very low frequency of  $10^{-5}$  Hz but it becomes significant and at the highest in this range specifically between  $10^{-4}$  and  $10^{-2}$  Hz while having a peak of 27.1% at  $10^{-3}$  Hz. In the middle range, the reduction in  $|E^*|$  decreased from 25.74% at  $10^{-2}$  Hz to 8.5% at  $10^{+2}$  Hz. In the higher frequency range, the reduction in  $|E^*|$  is almost constant and not significant ranging between 8.5% at  $10^{+2}$  Hz and 9.45% at  $10^{+5}$  Hz.

In the case of HMA mixtures with high RAP content (HR45), the reduction is significant and occurred also in the lower range of frequencies with a maximum  $|E^*|$  reduction of 27.85% at  $10^{-5}$  Hz. As  $f_r$  increases in the lower range, the reduction decreased reaching 16.7% at  $10^{-2}$  Hz. In the middle frequency range, the reduction in  $|E^*|$  decreased from 16.7% at  $10^{-2}$  Hz to 9.88% at  $10^{+2}$  Hz. In the higher frequency range, the reduction in

$|E^*|$  is almost constant and not significant ranging between 9.88% at  $10^{+2}$  Hz and 10.69% at  $10^{+5}$  Hz. As a summary, the reduction in  $|E^*|$  for HR15 and HR25 caused by Rediset addition is almost equal and higher than that of HR45 in the middle range of frequencies. In the higher  $f_r$  range, comparable reduction in  $|E^*|$  is found for different RAP mixtures assessed. Essentially, it was observed that the effect of Rediset on RAP mixtures was at the highest and mostly significant in the lower frequency range regardless of the RAP content incorporated. Knowing that the behavior of AC mixtures at low frequencies corresponds to its behavior at high temperature in which the rutting distress prevails, it is very critical to assess the impact of the significant reduction in  $|E^*|$  found on the rutting performance of WMA-RAP mixtures compared to standard RAP mixtures.

In addition, the reduction in  $|E^*|$  caused by Rediset additive in both the middle and higher range of frequencies indicates, respectively, an improvement in the fatigue and thermal cracking of WMA-RAP mixtures with respect to their corresponding HMA-RAP mixes.

### 3.3. Phase Angle Results

Figure 13 shows the phase angle mastercurves of diverse mixes of the study in semi-log scale. In the case of phase angle, the effect of the addition of Rediset was not consistent over the range of analyzed frequencies for RAP mixes unlike the case of the dynamic modulus. WR15 mix has the highest  $\Phi$  at smaller frequencies and at the lower band of middle frequency range indicating highest viscous behavior of this mix among others which correlates well with the lowest dynamic modulus associated to it. At the upper band of the middle range and at higher frequencies, comparable  $\Phi$  can generally be observed.

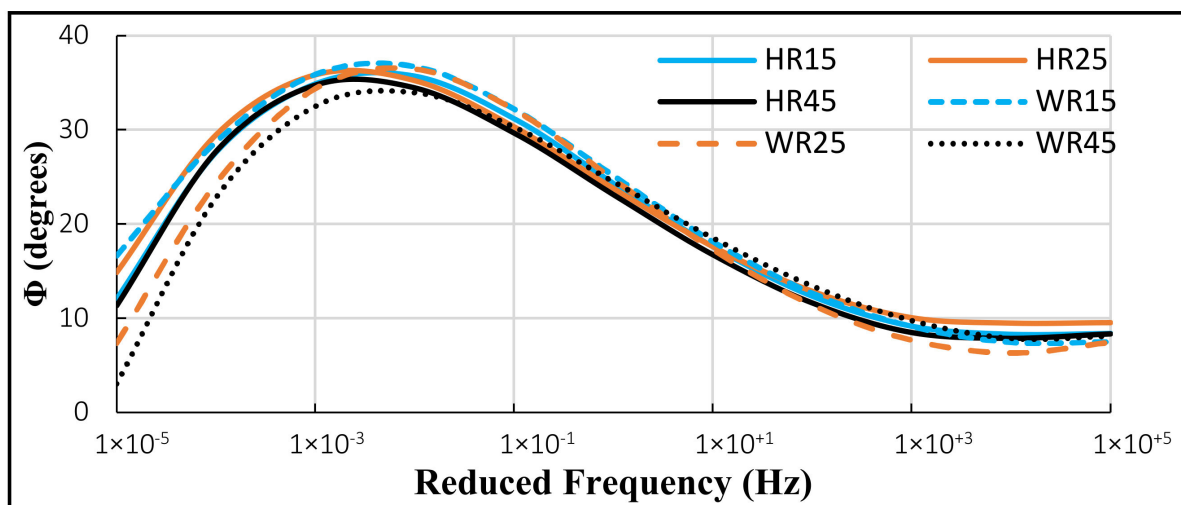
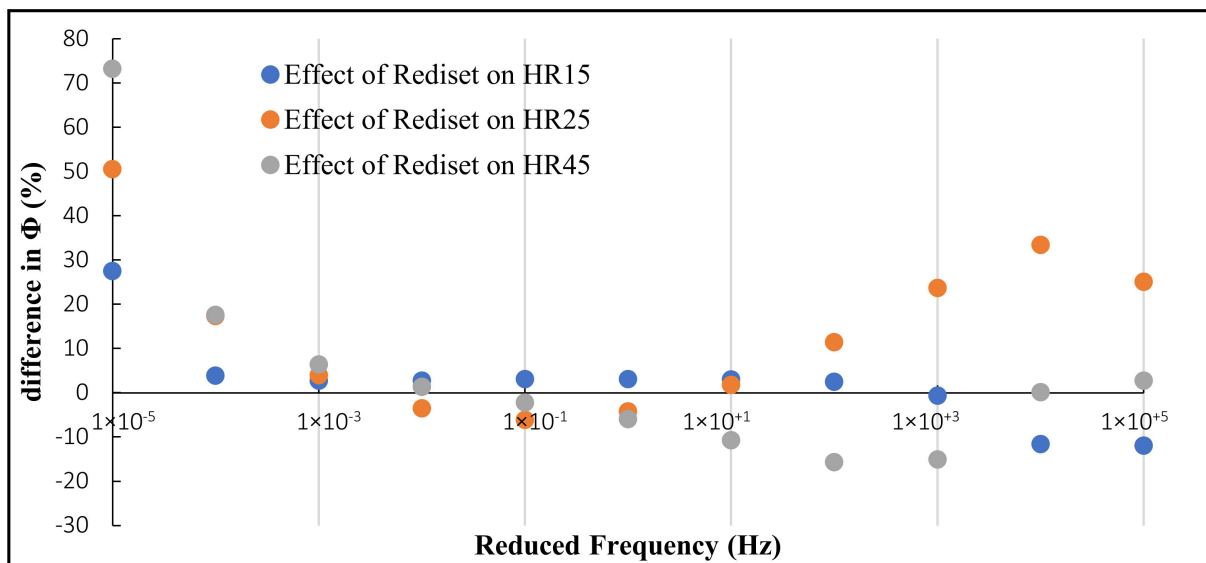


Figure 13. Phase angle mastercurves in semi-log scale.

#### Effect of Rediset on $\Phi$ According to RAP Content

In order to show the effect of Rediset on each RAP content separately, the difference (%) in  $\Phi$  between HR and its corresponding WR mix was plotted against the reduced frequency as illustrated by Figure 14.

For HMA mixtures incorporating low RAP content (HR15), Rediset addition increased  $\Phi$  values between  $f_r$  of  $10^{-5}$  and  $10^{+3}$  Hz and decreased  $\Phi$  values for  $f_r$  above  $10^{+3}$  Hz. Nevertheless, the only significant effect is observed at very low frequency of  $10^{-5}$  Hz. Moreover, a slight increase of about 2.87% in the peak value of  $\Phi$  is observed for WR15 compared to HR 15, while for both HR15 and WR15 mixes, the peak occurred approximately at the same reduced frequency level indicating that the maximum viscous effect occurs in both mixtures at the same temperature or at the same loading time.



**Figure 14.** Effect of Rediset on  $\Phi$  of mixtures with RAP.

For HMA mixtures incorporating medium RAP content (HR25), Rediset addition increased  $\Phi$  values for  $f_r$  under  $10^{-3}$  Hz, slightly decreased  $\Phi$  values between  $10^{-2}$  and  $10^{+1}$  Hz, and increased  $\Phi$  values again above  $10^{+1}$  Hz. However, the effect of Rediset is significant only at very low frequency of  $10^{-5}$  Hz and very high frequencies above  $10^{+4}$  Hz. An insignificant increase of 1.7% in the peak value of WR25 compared to HR25 is observed, while for this WR25 mix, the peak  $\Phi$  is reached at comparatively lower temperature (higher reduced frequency) than HR25, indicating development of peak viscous effect at relatively lower temperature for the AC mix.

Finally, for HMA mixtures incorporating high RAP content (HR45), Rediset addition increased  $\Phi$  values for  $f_r$  under  $10^{-2}$  Hz, decreased  $\Phi$  values for  $f_r$  between  $10^{-1}$  and  $10^{+3}$  Hz, and is ineffective on  $\Phi$  values for  $f_r$  above  $10^{+4}$  Hz. An insignificant decrease of 2.38% in the peak value of WR45 compared to HR45 is observed, while for this WR45 mix, the peak  $\Phi$  is reached at comparatively lower temperature (higher reduced frequency) than HR45, indicating development of peak viscous effect at relatively lower temperature for the AC mix.

### 3.4. Flow Number Results

Table 6 shows the results of FN testing for different HR and WR mixes and Figure 15 presents a graphical plot to compare both FN and FN index data. It is worth noting that the variation in the flow number FN test can be relatively high as the highest proportion of the coefficient of variation in FN-values was 28.97% for the mix HR45. The variation is even higher for the FN index calculation with a maximum COV value of 47.09% for HR45 as well.

**Table 6.** Summary of flow number (FN) test results.

#	AC Mix	Sample ID#	FN Cycles	$\epsilon_p$	FN Index
1	HR15	replicate #1	294.00	18,475.00	62.84
		replicate #2	271.00	19,203.00	70.86
		replicate #3	421.00	23,678.00	56.24
		Mean	328.67	20,452.00	62.23
		Std	80.79	2817.41	7.32
		COV (%)	24.58	13.78	11.76

Table 6. Cont.

#	AC Mix	Sample ID#	FN Cycles	$\epsilon_p$	FN Index
2	HR25	replicate #1	343.00	21,821.00	63.62
		replicate #2	479.00	21,128.00	44.11
		replicate #3	376.00	20,305.00	54.00
		Mean	399.33	21,084.67	53.91
		Std	70.94	758.93	9.76
		COV (%)	17.76	3.60	18.10
3	HR45	replicate #1	925.00	22,219.00	24.02
		replicate #2	569.00	29,816.00	52.40
		replicate #3	1037.00	26,391.00	25.45
		Mean	843.67	26,142.00	33.96
		Std	244.37	3804.62	15.99
		COV (%)	28.97	14.55	47.09
4	WR15	replicate #1	165.00	24,213.00	146.75
		replicate #2	130.00	25,190.00	193.77
		replicate #3	138.00	13,765.00	99.75
		Mean	144.33	21,056.00	146.75
		Std	18.34	6333.06	47.01
		COV (%)	12.71	30.08	32.03
5	WR25	replicate #1	224.00	22,186.00	99.04
		replicate #2	203.00	25,668.00	126.44
		replicate #3	184.00	24,231.00	131.69
		Mean	203.67	24,028.33	119.06
		Std	20.01	1749.82	17.53
		COV (%)	9.82	7.28	14.72
6	WR45	replicate #1	247.00	17,168.00	69.51
		replicate #2	181.00	24,764.00	136.82
		replicate #3	212.00	22,352.00	105.43
		Mean	213.33	21,428.00	103.92
		Std	33.02	3881.38	33.68
		COV (%)	15.48	18.11	32.41

From the analysis of the results both parameters indicate the same information, that WR mixes are more susceptible to rutting than HR mixes and by descending order, the rutting resistance of HR45 is the highest, then HR25, HR15, WR45, WR25, and finally WR15. Furthermore, it was found that the addition of Rediset reduced the FN of HR45 by 74.7%, HR25 by 49%, and HR 15 by 56%, and increased the FN index of HR 45, HR25, and HR15 by 136%, 121%, and 206%. Essentially, the results indicated that better rutting performance is associated to increased RAP content for both HMA-RAP and WMA-RAP mixtures. This can be explained by the fact that the RAP contains aged binder having higher PG grade that stiffen the mixture and is indeed contributing to an increase in the rutting resistance.

Ultimately, the results of Figure 15 indicates that despite the reduction in FN induced by the Rediset effect, both RAP and WMA-RAP mixes except WR15 provided acceptable level of rutting performance with a FN above 190 cycles [46].

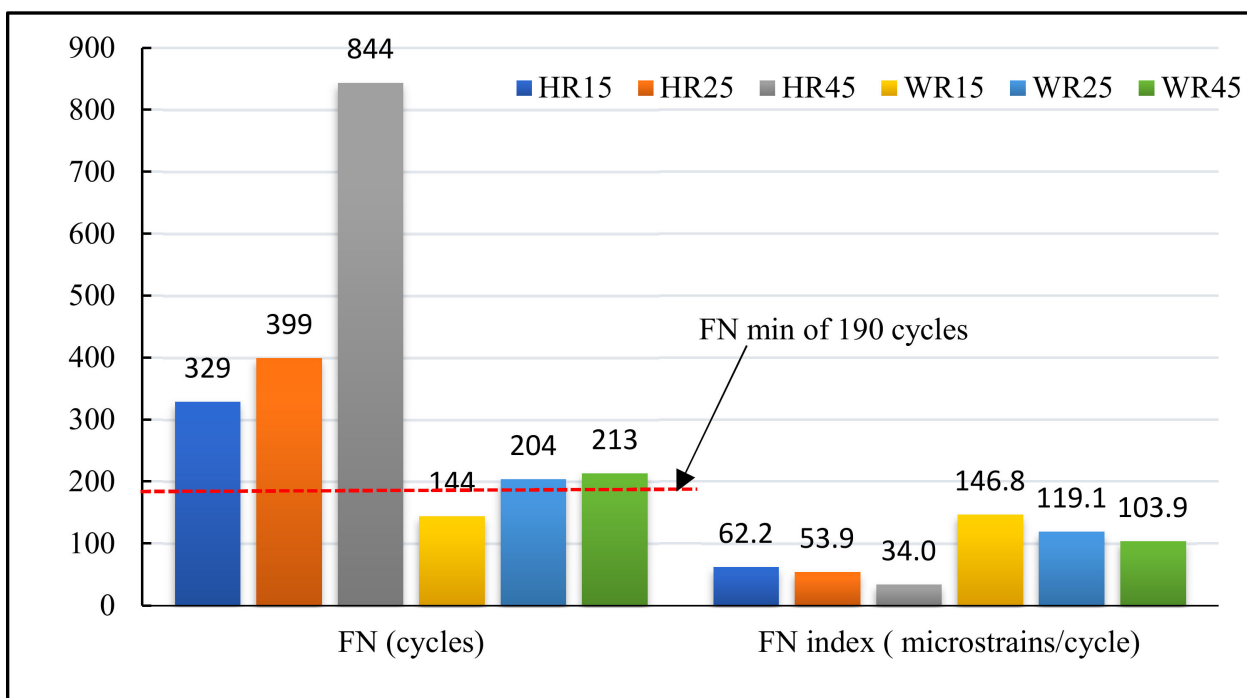


Figure 15. Graphical comparisons of FN results.

### 3.5. Comparison between $|E^*|$ and FN Test Results of Asphalt Mixtures

$|E^*|$  values at higher temperatures are generally used to evaluate the rutting performance since asphalt mixtures are susceptible to this distress at higher temperatures. In line with that,  $|E^*|$  values at higher temperatures 37.8 °C and 54 °C with different frequency levels of 25, 10, 5, 1, 0.5, and 0.1 Hz were acquired from the dynamic modulus mastercurve of each mixture. Tables 7 and 8 show the results of  $|E^*|$  at the investigated temperature/frequency condition versus the FN results for the mixtures of the study.

Table 7.  $E^*|$  at 37.8 °C vs. FN results.

Mix	$ E _{37.8^\circ C, 25 Hz}$	Rank	$ E _{37.8^\circ C, 10 Hz}$	Rank	$ E _{37.8^\circ C, 5 Hz}$	Rank	$ E _{37.8^\circ C, 1 Hz}$	Rank	$ E _{37.8^\circ C, 0.5 Hz}$	Rank	$ E _{37.8^\circ C, 0.1 Hz}$	Rank	FN Rank
HR15	3608.02	3	2700.77	3	2128.92	3	1159.58	3	875.73	2	426.36	3	3
HR25	3640.78	2	2730.56	2	2152.96	2	1163.96	2	871.54	3	445.03	2	2
HR45	4164.06	1	3160.14	1	2513.53	1	1382.48	1	1040.28	1	509.88	1	1
WR15	2844.59	6	2071.90	6	1599.90	6	834.54	6	621.03	6	309.32	6	6
WR25	3172.39	5	2325.44	5	1802.19	5	943.12	5	701.04	5	346.21	5	5
WR45	3383.45	4	2514.49	4	1965.24	4	1033.22	4	761.62	4	355.99	4	4

Table 8.  $E^*|$  at 54 °C vs. FN results.

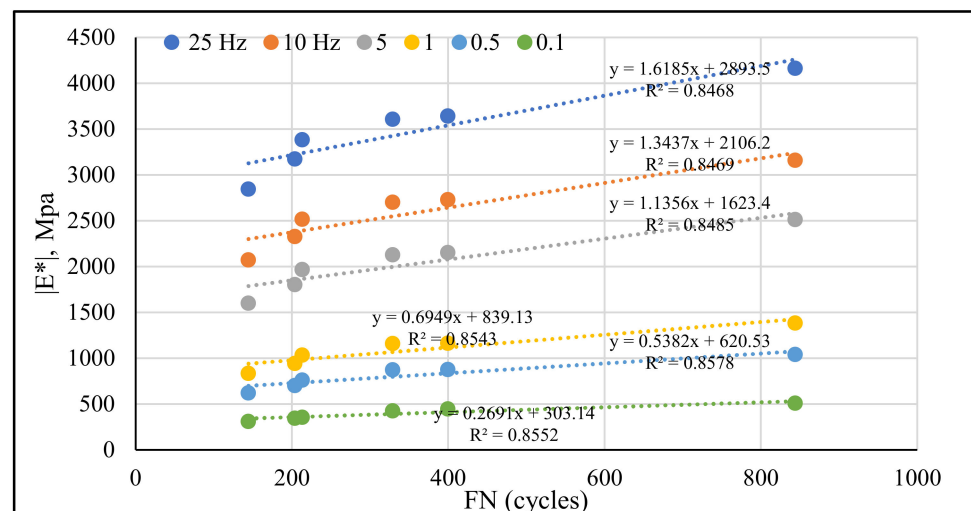
Mix	$ E _{54^\circ C, 25 Hz}$	Rank	$ E _{54^\circ C, 10 Hz}$	Rank	$ E _{54^\circ C, 5 Hz}$	Rank	$ E _{54^\circ C, 1 Hz}$	Rank	$ E _{54^\circ C, 0.5 Hz}$	Rank	$ E _{54, 0.1 Hz}$	Rank	FN Rank
HR15	1299.79	3	890.44	3	691.78	2	349.56	2	260.83	2	135.59	1	3
HR25	1330.47	2	922.09	2	659.17	3	316.78	3	229.15	3	108.38	3	2
HR45	1604.68	1	112.56	1	837.95	1	402.75	1	289.40	1	132.36	2	1
WR15	896.56	6	603.91	6	445.51	6	253.15	4	189.15	4	100.25	4	6
WR25	100.56	5	673.89	5	487.53	5	220.91	5	165.10	5	88.102	5	5
WR45	1013.10	4	684.201	4	507.43	4	220.44	6	155.18	6	68.832	6	4

It can be concluded from Table 7 that at a temperature of 37.8 °C, DM and FN provide mostly similar ranking of the rutting performance of asphalt mixtures. However, as illustrated in Table 8, at a temperature of 54 °C only at higher frequencies of 25 and 10 Hz, the ranking of rutting performance of DM and FN is comparable. At a temperature of 54 °C and a frequency 5 Hz, DM ranks the rutting resistance of HR15 higher than HR 25 compared

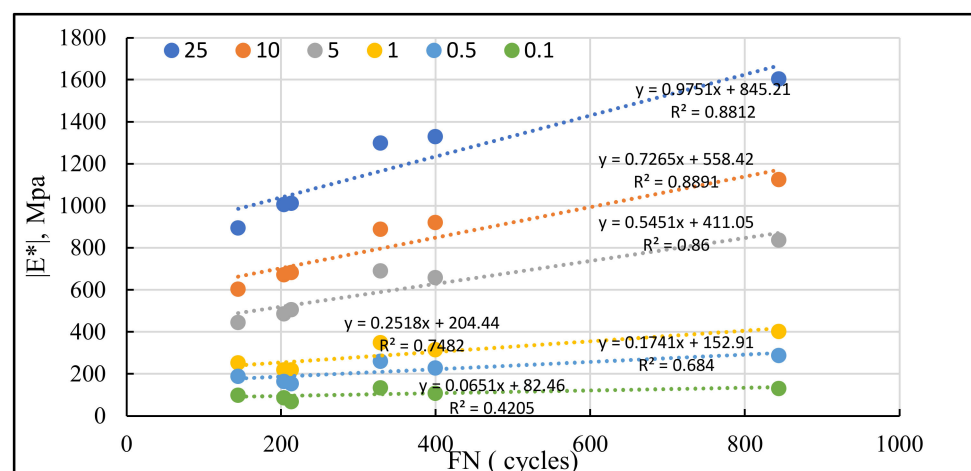
to FN. An additional difference is observed between DM and FN at a temperature of 54 °C for smaller frequencies, especially at 0.1 Hz, where DM ranks, respectively, HR15 and WR45 as the highest and lowest resistant mixes to rutting whereas FN ranks HR 45 and WR15 as the highest and lowest resistant mixes to rutting.

#### Graphical Correlations for the Laboratory Results

The results of the correlations in Figure 16a reveal that at a temperature of 37.8 °C at which both the dynamic modulus (DM) and flow number (FN) present comparable ranking of the rutting potential of asphalt mixtures, strong correlations ( $R^2 > 0.84$ ) existed between  $|E^*|$  and (FN) results, the best correlation being found at a frequency of 0.5 Hz and 0.1 Hz. At a temperature of 54 °C, it is observed in Figure 16b that there are no strong correlations between the flow number (FN) and  $|E^*|$  values ( $R^2 < 0.75$ ) for frequencies of 1 Hz and below, however, strong correlations were found between the FN and  $|E^*|$  values for higher frequencies of 5, 10, and 25 Hz ( $R^2 > 0.86$ ). Based on the findings of this section, and since the NCHRP 465 reported a strong correlation between FN results and rutting measured in field [38],  $|E^*|$  at 37.8 °C and especially for 0.1 Hz (highest  $R^2 = 0.857$ ) or at 54 °C and for a frequency of 10 Hz (highest  $R^2 = 0.889$ ) might be a proper DM laboratory test condition for estimating the rutting-resistance potential of RAP and WMA-RAP mixes in the field.



(a)



(b)

Figure 16. Correlations between FN and  $|E^*|$  at (a) 37.8 °C, (b) 54 °C.

#### 4. Conclusions and Recommendations

In order to evaluate the effect of Rediset additive on the performance of RAP mixtures, two commonly used laboratory performance tests, DM and FN, were conducted on six asphalt mixes incorporating different RAP contents. The main findings of this study are listed as follows:

- The addition of Rediset WMA additive reduces  $|E^*|$  of the corresponding RAP mix at both high and low reduced frequencies. Nevertheless, the reduction is mostly significant in the lower frequency range.
- The higher is the RAP content the higher is the  $|E^*|$  of the mixture for both RAP and WMA-RAP technology, and along the frequency axis  $|E^*|$  of RAP mixes with low, medium, and high RAP content are mostly higher than WMA-RAP mixes.
- The Rediset additive improved the fatigue and thermal cracking of WMA-RAP mixtures with respect to their corresponding RAP mixes. On the other hand, the rutting resistance was reduced due to Rediset. Yet, it was acceptable for all mixes except the mix incorporating low RAP content of 15%.
- In the case of phase angle, the effect of the addition of Rediset was not consistent over the range of analyzed frequencies for RAP mixes. For HMA mixtures incorporating low RAP content (HR15), the only significant effect of Rediset addition (increase in  $\Phi$ ) is observed at very low frequency of  $10^{-5}$  Hz, above which comparable values of phase angle between RAP and WMA-RAP mix are obtained.
- For HMA mixtures incorporating medium RAP content (HR25), a significant effect of Rediset addition (increase in  $\Phi$ ) is observed at very low frequency of  $10^{-5}$  Hz and higher frequencies above  $10^{+4}$  Hz, while comparable values of phase angles for RAP and WMA-RAP mix are obtained in the range between these frequencies.
- Regarding HMA mixtures incorporating high RAP content (HR45), Rediset addition increased  $\Phi$  values mostly for  $f_r$  under  $10^{-2}$  Hz while for other frequencies, comparable phase angle values for RAP and WMA-RAP mixes can be expected.
- $|E^*|$  at 37.8 °C and especially for 0.1 Hz or at 54 °C and for a frequency of 10 Hz might be a proper DM test condition for estimating the rutting-resistance potential of RAP and WMA-RAP mixes in the field.

The findings revealed by this study can be elaborated by further investigation in areas that may include:

1. The effect of WMA additive on asphaltic mixtures incorporating RAP content exceeding 50%, 75%, and even 100% recyclable mixtures.
2. Assessing the impact of using vegetable, organic, or petroleum rejuvenator combined with the WMA additive on the properties and performance of HMA-RAP mixture.
3. Examination of the variation in the particle size distribution of the extracted recycled aggregates for mixtures produced using different RAP percentages.

**Author Contributions:** Conceptualization, F.B.; methodology, F.B.; validation, J.K. and A.C.; formal analysis, F.B. and J.K.; investigation, F.B.; resources, F.B.; data curation, F.B. and A.C.; writing—original draft preparation, F.B.; writing—review and editing, J.K. and A.C.; visualization, F.B.; supervision, J.K. and A.E.; project administration, A.E. All authors have read and agreed to the published version of the manuscript.

**Funding:** This research received no external funding.

**Institutional Review Board Statement:** Not applicable.

**Informed Consent Statement:** No applicable.

**Data Availability Statement:** Data sharing not applicable.

**Acknowledgments:** The authors of this manuscript appreciate the contribution of Hussein Kassem who provided us with useful information that helped in the completion of this study.

**Conflicts of Interest:** The authors declare no conflict of interest.

## References

1. Prowell, B.D.; Hurley, G.C.; Frank, B. *Warm-Mix Asphalt: Best Practices*; National Asphalt Pavement Association: Lanham, MD, USA, 2011.
2. Kanitpong, K.; Nam, K.; Martono, W.; Bahia, H. Evaluation of a warm-mix asphalt additive. *Proc. Inst. Civ. Eng.-Constr. Mater.* **2008**, *161*, 1–8. [[CrossRef](#)]
3. Dos Santos, S.; Partl, M.N.; Poulikakos, L.D. From virgin to recycled bitumen: A microstructural view. *Compos. Part B Eng.* **2015**, *80*, 177–185. [[CrossRef](#)]
4. Capitão, S.D.; Picado-Santos, L.G.; Martinho, F. Pavement engineering materials: Review on the use of warm-mix asphalt. *Constr. Build. Mater.* **2012**, *36*, 1016–1024. [[CrossRef](#)]
5. Kassem, H.A.; Chehab, G.R. Characterizing the behavior of warm mix asphalt using a visco-elasto-plastic continuum damage model. In *Advances in Materials and Pavement Prediction: Papers from the International Conference on Advances in Materials and Pavement Performance Prediction (AM3P 2018), April 16–18, 2018, Doha, Qatar*; CRC Press: Boca Raton, FL, USA, 2018; p. 101.
6. Kassem, H.A.; Chehab, G.R. Characterisation of the mechanical performance of asphalt concrete mixtures with selected WMA additives. *Int. J. Pavement Eng.* **2021**, *22*, 625–642. [[CrossRef](#)]
7. Li, Q.; Li, G.; Ma, X.; Zhang, S. Linear viscoelastic properties of warm-mix recycled asphalt binder, mastic, and fine aggregate matrix under different aging levels. *Constr. Build. Mater.* **2018**, *192*, 99–109. [[CrossRef](#)]
8. Chen, Y.; Chen, Z.; Xiang, Q.; Qin, W.; Yi, J. Research on the influence of RAP and aged asphalt on the performance of plant-mixed hot recycled asphalt mixture and blended asphalt. *Case Stud. Constr. Mater.* **2021**, *15*, e00722. [[CrossRef](#)]
9. Barra, Firas and Elkordi, Adel, Assessment of Dynamic Modulus and Prediction of Phase Angle of Conventional and Reclaimed Asphalt Mixtures Incorporating Different Rap Contents. Available online: <https://ssrn.com/abstract=4035377> or <http://dx.doi.org/10.2139/ssrn.4035377> (accessed on 25 April 2022).
10. Kaseer, F.; Martin, A.E.; Arámbula-Mercado, E. Use of recycling agents in asphalt mixtures with high recycled materials contents in the United States: A literature review. *Constr. Build. Mater.* **2019**, *211*, 974–987. [[CrossRef](#)]
11. He, G.P.; Wong, W.G. Effects of moisture on strength and permanent deformation of foamed asphalt mix incorporating RAP materials. *Constr. Build. Mater.* **2008**, *22*, 30–40. [[CrossRef](#)]
12. Monu, K.; Ransinchung, G.D.; Singh, S. Effect of long-term ageing on properties of RAP inclusive WMA mixes. *Constr. Build. Mater.* **2019**, *206*, 483–493. [[CrossRef](#)]
13. Farooq, M.A.; Mir, M.S. Use of reclaimed asphalt pavement (RAP) in warm mix asphalt (WMA) pavements: A review. *Innov. Infrastruct. Solut.* **2017**, *2*, 10. [[CrossRef](#)]
14. Oliveira, J.R.; Silva, H.M.; Abreu, L.P.; Gonzalez-Leon, J.A. The role of a surfactant based additive on the production of recycled warm mix asphalts—Less is more. *Constr. Build. Mater.* **2012**, *35*, 693–700. [[CrossRef](#)]
15. Gungat, L.; Yusoff, N.I.M.; Hamzah, M.O. Effects of RH-WMA additive on rheological properties of high amount reclaimed asphalt binders. *Constr. Build. Mater.* **2016**, *114*, 665–672. [[CrossRef](#)]
16. Zhao, S.; Huang, B.; Shu, X.; Jia, X.; Woods, M. Laboratory performance evaluation of warm-mix asphalt containing high percentages of reclaimed asphalt pavement. *Transp. Res. Rec.* **2012**, *2294*, 98–105. [[CrossRef](#)]
17. Xie, Z.; Tran, N.; Taylor, A.; Julian, G.; West, R.; Welch, J. Evaluation of foamed warm mix asphalt with reclaimed asphalt pavement: Field and laboratory experiments. *Road Mater. Pavement Des.* **2017**, *18* (Suppl. 4), 328–352. [[CrossRef](#)]
18. Behbahani, H.; Ayazi, M.J.; Moniri, A. Laboratory investigation of rutting performance of warm mix asphalt containing high content of reclaimed asphalt pavement. *Pet. Sci. Technol.* **2017**, *35*, 1556–1561. [[CrossRef](#)]
19. Lu, D.X.; Saleh, M. Laboratory evaluation of warm mix asphalt incorporating high rap proportion by using evotherm and sylvaroad additives. *Constr. Build. Mater.* **2016**, *114*, 580–587. [[CrossRef](#)]
20. Guo, N.; You, Z.; Tan, Y.; Zhao, Y. Performance evaluation of warm mix asphalt containing reclaimed asphalt mixtures. *Int. J. Pavement Eng.* **2017**, *18*, 981–989. [[CrossRef](#)]
21. Kim, D.; Norouzi, A.; Kass, S.; Liske, T.; Kim, Y.R. Mechanistic performance evaluation of pavement sections containing RAP and WMA additives in Manitoba. *Constr. Build. Mater.* **2017**, *133*, 39–50. [[CrossRef](#)]
22. El Sharkawy, S.A.; Wahdan, A.H.; Galal, S.A. Utilisation of warm-mix asphalt technology to improve bituminous mixtures containing reclaimed asphalt pavement. *Road Mater. Pavement Des.* **2017**, *18*, 477–506. [[CrossRef](#)]
23. Valdes-Vidal, G.; Calabi-Floody, A.; Sanchez-Alonso, E. Performance evaluation of warm mix asphalt involving natural zeolite and reclaimed asphalt pavement (RAP) for sustainable pavement construction. *Constr. Build. Mater.* **2018**, *174*, 576–585. [[CrossRef](#)]
24. Das, P.K.; Tasdemir, Y.; Birgisson, B. Low temperature cracking performance of WMA with the use of the Superpave indirect tensile test. *Constr. Build. Mater.* **2012**, *30*, 643–649. [[CrossRef](#)]
25. Ghabchi, R.; Singh, D.; Zaman, M. Laboratory evaluation of stiffness, low-temperature cracking, rutting, moisture damage, and fatigue performance of WMA mixes. *Road Mater. Pavement Des.* **2015**, *16*, 334–357. [[CrossRef](#)]
26. Vaitkus, A.; Čygas, D.; Laurinavičius, A.; Vorobjovas, V.; Perveneckas, Z. Influence of warm mix asphalt technology on asphalt physical and mechanical properties. *Constr. Build. Mater.* **2016**, *112*, 800–806. [[CrossRef](#)]
27. Singh, D.; Ashish, P.K.; Chitragar, S.F. Laboratory performance of recycled asphalt mixes containing wax and chemical based warm mix additives using semi circular bending and tensile strength ratio tests. *Constr. Build. Mater.* **2018**, *158*, 1003–1014. [[CrossRef](#)]

28. Frigio, F.; Canestrari, F. Characterisation of warm recycled porous asphalt mixtures prepared with different wma additives. *Eur. J. Environ. Civ. Eng.* **2016**, *22*, 82–98. [[CrossRef](#)]
29. Guo, N.; You, Z.; Zhao, Y.; Tan, Y.; Diab, A. Laboratory performance of warm mix asphalt containing recycled asphalt mixtures. *Constr. Build. Mater.* **2014**, *64*, 141–149. [[CrossRef](#)]
30. Hamzah, M.O.; Golchin, B.; Jamshidi, A.; Chailleux, E. Evaluation of Rediset for use in warm-mix asphalt: A review of the literatures. *Int. J. Pavement Eng.* **2015**, *16*, 809–831. [[CrossRef](#)]
31. Kassem, H.A.; Chehab, G.R.; Saleh, N.F.; Zalgout, A. Assessment of fiber reinforced HMA and WMA mixes using viscoelastic continuum damage model. In *Bearing Capacity of Roads, Railways and Airfields*; CRC Press: Boca Raton, FL, USA, 2017; pp. 1197–1204.
32. Liu, Y.; Wang, H.; Tighe, S.L.; Zhao, G.; You, Z. Effects of preheating conditions on performance and workability of hot in-place recycled asphalt mixtures. *Constr. Build. Mater.* **2019**, *226*, 288–298. [[CrossRef](#)]
33. McDaniel, R.; Anderson, R.M. *Recommended Use of Reclaimed Asphalt Pavement in the Superpave Mix Design Method: Technician's Manual*; NCHRP Report No. 452; Transportation Research Board: Washington, DC, USA, 2001.
34. Abed, A.; Thom, N.; Lo Presti, D. Design considerations of high RAP-content asphalt produced at reduced temperatures. *Mater. Struct.* **2018**, *51*, 91. [[CrossRef](#)]
35. Design, S.M. *Superpave Series No. 2 (SP-2)*; Asphalt Institute: Lexington, KY, USA, 1996.
36. Bonaquist, R. *Mix Design Practices for Warm Mix Asphalt*; NCHRP Report 691; Technologies, LLC.: Westborough, MA, USA, 2011.
37. Witzcak, M.W. *Simple Performance Tests: Summary of Recommended Methods and Database*; Transportation Research Board: Washington, DC, USA, 2005; Volume 46.
38. Witzcak, M.W. *Simple Performance Test for Superpave Mix Design*; Transportation Research Board: Washington, DC, USA, 2002; Volume 465.
39. Underwood, B.S.; Kim, Y.R. Comprehensive evaluation of small strain viscoelastic behavior of asphalt concrete. *J. Test. Eval.* **2012**, *40*, 622–632. [[CrossRef](#)]
40. Kim, Y.R.; Lee, Y.C. Interrelationships among Stiffnesses of Asphalt Aggregate Mixtures. *J. Assoc. Asph. Paving Technol.* **1995**, *64*, 575–610.
41. Booij, H.C.; Thoone, G.P.J.M. Generalization of Kramers-Kronig transforms and some approximations of relations between viscoelastic quantities. *Rheol. Acta* **1982**, *21*, 15–24. [[CrossRef](#)]
42. Yang, X.; You, Z. New predictive equations for dynamic modulus and phase angle using a nonlinear least-squares regression model. *J. Mater. Civ. Eng.* **2015**, *27*, 04014131. [[CrossRef](#)]
43. TxDOT (Texas Department of Transport). *Standard Specifications for Construction and Maintenance of Highways, Streets, and Bridges*; TxDOT: Austin, TX, USA, 2004.
44. Biligiri, K.; Kaloush, K.E.; Mamlouk, M.S.; Witzcak, M.W. Rational Modeling of Tertiary Flow for Asphalt Mixtures. Paper 07-0344, Annual Meeting of the Transportation Research Board CD ROM Compendium of Papers. *Transp. Res. Rec.* **2007**, *2001*, 63–72. [[CrossRef](#)]
45. Zhang, J.; Alvarez, A.E.; Lee, S.I.; Torres, A.; Walubita, L.F. Comparison of flow number, dynamic modulus, and repeated load tests for evaluation of HMA permanent deformation. *Constr. Build. Mater.* **2013**, *44*, 391–398. [[CrossRef](#)]
46. *AASHTO T 378*; Standard Method of Test for Determining the Dynamic Modulus and Flow Number for Asphalt Mixtures Using the Asphalt Mixture Performance Tester (AMPT). American Association of State Highway and Transportation Officials, 2017. Available online: [https://global.ihs.com/doc\\_detail.cfm?document\\_name=AASHTO%20T%20378&item\\_s\\_key=00730855](https://global.ihs.com/doc_detail.cfm?document_name=AASHTO%20T%20378&item_s_key=00730855) (accessed on 1 May 2022).